Single Image Dehazing Using Color Attenuation Prior

Qingsong Zhu[1]
qs.zhu@siat.ac.cn
Jiaming Mai[1, 2]
jiamingmai@163.com
Ling Shao[3]
ling.shao@ieee.org

[1] Shenzhen Institutes of Advanced Technology, Chinese Academy of Sciences, Shenzhen, China
[2] South China Agricultural University, Guangzhou, China
[3] Department of Electronic and Electrical Engineering, University of Sheffield, Sheffield, UK

Abstract

In this paper, we propose a simple but powerful prior, color attenuation prior, for haze removal from a single input hazy image. By creating a linear model for modelling the scene depth of the hazy image under this novel prior and learning the parameters of the model by using a supervised learning method, the depth information can be well recovered. With the depth map of the hazy image, we can easily remove haze from a single image. Experimental results show that the proposed approach is highly efficient and it outperforms state-of-the-art haze removal algorithms in terms of the dehazing effect as well.

1 Introduction

Outdoor images taken in bad weather (e.g., foggy or hazy) usually lose contrast and fidelity, resulting from the fact that light is absorbed and scattered by the turbid medium such as particles and water droplets in the atmosphere during the process of propagation. Moreover, most automatic systems, which strongly depend on the definition of the input images, fail to work normally caused by the degraded images. Therefore, image dehazing as a pre-processing restoration [1, 2, 3] step will benefit various algorithms that require image/video analysis.

Since the density of the haze is different from place to place and it is hard to detect in the hazy image, image dehazing is a challenging task. Early researchers use the traditional techniques of image processing to remove the haze from a single image (for instance, histogram-based dehazing methods [4, 5, 6]). However, the dehazing effect is limited, because a single hazy image can hardly provide much information. Later, researchers try to improve the dehazing effect with multiple images. In [7, 8], polarization-based methods are used for dehazing with multiple images which are taken with different degrees of polarization. Narasimhan et al. [9, 10, 11] propose haze removal approaches with multiple images of the same scene under different weather conditions. In [12, 13], dehazing is conducted based on the given depth information.

Recently, significant progress has been made in single image dehazing based on the

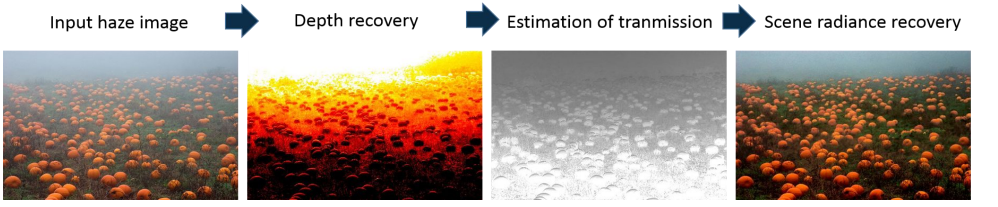

Figure 1: An overview of the proposed dehazing method.

physical model. Under the assumption that the local contrast of the haze-free image is much higher than that in the hazy image, Tan [14] propose a novel haze removal method by maximizing the local contrast of the image based on Markov Random Field (MRF). Although Tan's approach is able to achieve impressive results, it tends to produce over-saturated images. Fattal [15] propose to remove haze from color images based on Independent Component Analysis (ICA), but the approach is time-consuming and cannot be used for grayscale image dehazing. Furthermore, it has some difficulties to deal with the dense-haze images. Based on a large amount of observations on haze-free images, He et al. [16, 17] find the dark channel prior (DCP) that, in most of the non-sky patches, at least one color channel has some pixels whose intensities are very low and close to zero. With the help of this prior knowledge, they eliminate the distribution of the thickness of haze, and then recover the haze-free image by the atmospheric scattering model. The DCP approach is simple and effective in most cases. However, it cannot well handle the sky images and is computationally intensive. An improved algorithm, guided image filtering, is proposed in [21, 22] to substitute the time-consuming soft matting [20] used in [16, 17] later. Assuming that the depth of the scene is continuous, Tarel et al. [21] introduce a fast dehazing approach based on the median filter. Unfortunately, this algorithm cannot be used on all hazy images because such a strong assumption is violated in some cases. Moreover, it is not adaptive as too many parameters need to be controlled in the approach. Nishino et al. [22, 23] propose a probabilistic dehazing method, which models the image with a factorial Markov Random Filed to estimate the scene radiance and the depth information. This approach can recover most details from the hazy image, but the result suffers from oversaturation.

In this paper, we propose a novel color attenuation prior for image dehazing. This simple and powerful prior can help to create a linear model for the scene depth of the hazy image. By learning the parameters of the linear model with a supervised learning method, the bridge between the hazy image and its corresponding depth map is built effectively. With the recovered depth information, we can easily remove the haze from the single hazy image. An overview of the proposed dehazing method is shown in Figure 1. The efficiency of this dehazing method is dramatically high and the dehazing effect is also superior to that of popular dehazing algorithms as we will show in Section 5.

The remainder of this paper is organized as follows: In Section 2, we review the atmospheric scattering model which is widely used for image dehazing and give a concise analysis on the parameters of this model. In Section 3, we discuss the proposed approach of recovering the scene depth using the color attenuation prior. In Section 4, the method of image dehazing with the depth information is described. In Section 5, we present and analyse the experimental results. Finally, we summarize this paper in Section 6.

2 Atmospheric scattering model

To describe the formation of a hazy image, the atmospheric scattering model, which was proposed by McCartney in 1976 [24], is widely used in computer vision and image processing. Narasimhan and Nayar [10, 25] further derive the model later, and the model can be expressed as follows:

$$\mathbf{I}(x) = \mathbf{J}(x)t(x) + \mathbf{A}(1 - t(x)) \tag{1}$$

$$t(x) = \mathrm{e}^{-\beta d(x)} \tag{2}$$

where **I** is the hazy image, **J** is the scene radiance representing the haze-free image, **A** is the atmospheric light, t is the medium transmission, β is the scattering coefficient of the atmosphere and d is the depth of scene. Since **I** is known, the goal of dehazing is to eliminate **A** and t, then restore **J** according to Equation (1).

We notice that the depth of the scene d is the most important information. On the one hand, since the scattering coefficient β can be regarded as a constant, the medium transmission t can be estimated easily if the depth of the scene is given according to Equation (2). On the other hand, when the depth $d(x)$ tends to infinity, the transmission $t(x)$ tends to zero and we have:

$$\mathbf{I}(x) = \mathbf{A},\ d(x) \to \infty \tag{3}$$

Equation (3) shows that the intensity of the pixel, which makes the depth d tend to infinity, can stand for the value of the atmospheric light **A**. In this condition, the task of dehazing can be further converted into depth information recovery. However, it is a challenging task to obtain the depth map with a single hazy image.

In the next section, we present a novel approach to recover the depth information directly for a single hazy image.

3 Scene depth recovery

3.1 Color attenuation prior

Haze is traditionally an atmospheric phenomenon in which smoke, dust and other dry particles obscure the clarity of the scenery objects. Environmental illumination tends to be scattered by this kind of turbid medium and the white airlight is formed. It turns out that images taken in such bad weather are often much brighter and the color of the scenery object fades in different degree. The brightness of the pixels within the hazy image becomes much higher than that in the real scene, and the saturation of these pixels is pretty low. In this context, regions with haze are characterized by high brightness and low saturation. We believe that this cannot be coincidence and do a lot of experiments on the hazy images to find the statistics and seek a novel prior for image dehazing. The main conclusion is that the density of the haze is positively correlated with the difference between the brightness and the saturation. We illustrate this in Figure 2. Since the haze density increases along with the change of scene depth in general, we can make an assumption that the depth of the scene is positively correlated with the density of the haze and we have:

$$d(x) \propto c(x) \propto v(x) - s(x) \tag{4}$$

where d is the scene depth, c is the haze density, v is the brightness of the scene and s is the saturation. We regard this statistics as color attenuation prior. Although we have

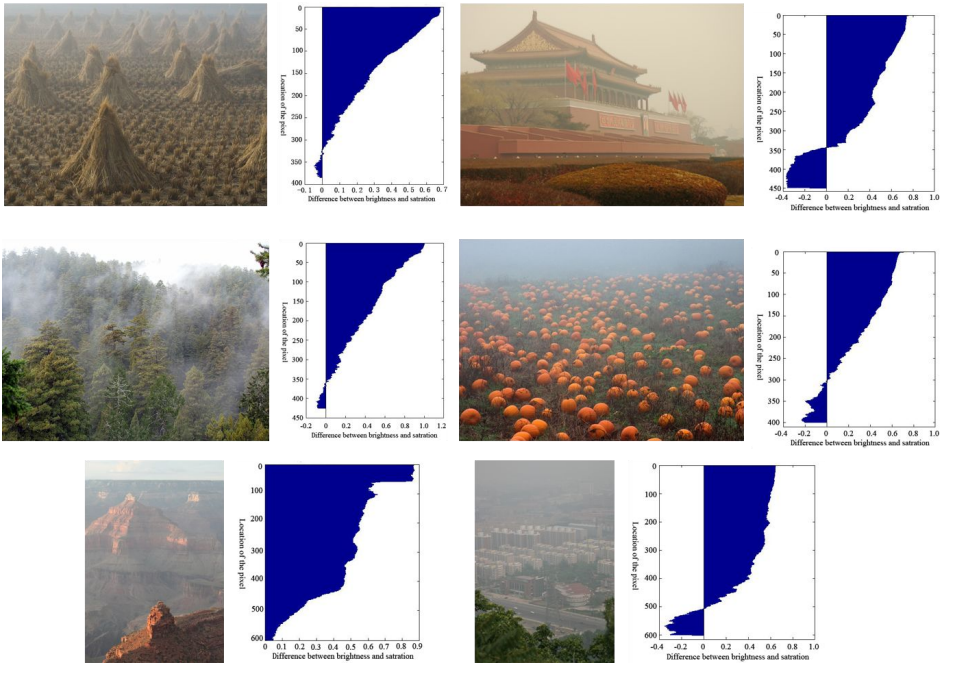

Figure 2: Hazy images and their corresponding histograms of the difference between brightness and saturation.

known that there must be some links among d, v and s, Equation (4) is just an intuitional result of the observation and it cannot be an accurate expression.

3.2 Color attenuation prior

As the difference between the brightness and the saturation can approximately represent the density of the haze (see Figure 2), we boldly assume that the relationship among the scene depth d, the brightness v and the saturation s is linear. Based on this assumption, we can create a linear model as follows:

$$d(x) = \theta_0 + \theta_1 v(x) + \theta_2 s(x) \tag{5}$$

where d is the scene depth, v is the brightness, s is the saturation, and (θ_0 , θ_1 , θ_2) are the unknown linear coefficients. Although the definition of the scene depth d has been given by Equation (5), the rationality of the assumption has not been validated. To answer the question why the relationship among d, v and s is linear in our model, we calculate the gradient of d in Equation (5) and we have:

$$\nabla d = \theta_1 \nabla v + \theta_2 \nabla s \tag{6}$$

Since v and s are actually the two single-channel images (the brightness channel and the saturation channel of the HSB color space) into which the hazy image $\mathbf{I}$ split, Equation (6) ensures that d has an edge only if $\mathbf{I}$ has an edge**.** In other words, the linear model has the important edge-preserving property, which makes sure that the depth information can be well recovered even near the depth discontinuities in the scene. This linear model works really well as we will show later.

In the next section, we use a simple and efficient supervised learning method to determine the coefficients (θ_0 , θ_1 , θ_2).

3.3 Learning strategy for the linear coefficients

In order to learn the coefficients (θ_0 , θ_1, θ_2) accurately, the training data are necessary. A training sample consists of a hazy image and its corresponding ground truth depth map in our case. To seek a solution that minimizes the difference between the scene depth $d(x)$ estimated by Equation (4) and the true depth, we minimize the following squared loss function:

$$L = \frac{1}{n|\omega|}\sum_{i=1}^{n}\sum_{j=1}^{\omega_i}(d_{ri}(x_j) - (\theta_0 + \theta_1 v_i(x_j) + \theta_2 s_i(x_j)))^2 \tag{7}$$

Here, n is the number of the training samples, ω_i is the size of the hazy image of the ith training sample, $|\omega|$ is the total number of the pixels of all the hazy images in the training set, d_{ri} is the depth map of the ith training sample, v_i and s_i are the brightness channel and the saturation channel of the hazy image of the ith training sample respectively.

The problem of estimating the linear coefficients (θ_0 , θ_1 , θ_2) can be converted into the problem of solving the following equations:

$$\begin{cases} \dfrac{\partial L}{\partial \theta_0} = \dfrac{2}{n|\omega|}(\theta_0 \mathrm{n}|\omega| + \theta_1\sum_{i=1}^{n}\sum_{j=1}^{\omega_i} v_i(x_j) + \theta_1\sum_{i=1}^{n}\sum_{j=1}^{\omega_i} s_i(x_j) - \sum_{i=1}^{n}\sum_{j=1}^{\omega_i} d_{ri}(x_j)] = 0 \\ \dfrac{\partial L}{\partial \theta_1} = \dfrac{2}{n|\omega|}\sum_{i=1}^{n}\sum_{j=1}^{\omega_i}[\theta_0 v_i(x_j) + \theta_1 v_i^2(x_j) + \theta_2 v_i(x_j)s_i(x_j) - v_i(x_j)d_{ri}(x_j)] = 0 \\ \dfrac{\partial L}{\partial \theta_2} = \dfrac{2}{n|\omega|}\sum_{i=1}^{n}\sum_{j=1}^{\omega_i}[\theta_0 s_i(x_j) + \theta_1 s_i^2(x_j) + \theta_2 v_i(x_j)s_i(x_j) - s_i(x_j)d_{ri}(x_j)] = 0 \end{cases} \tag{8}$$

To facilitate the calculation, we first define the two matrices $\mathbf{X}$ and $\boldsymbol{\theta}$, and combine all the d_{ri} into a vector $\mathbf{D}$ as follows:

$$\mathbf{X} = \begin{bmatrix} 1 & v_1 & s_1 \\ 1 & v_2 & s_2 \\ \vdots & \vdots & \vdots \\ 1 & v_n & s_n \end{bmatrix} \quad \boldsymbol{\theta} = \begin{bmatrix} \theta_0 \\ \theta_1 \\ \theta_2 \end{bmatrix} \quad \mathbf{D} = \begin{bmatrix} d_{r1} \\ d_{r2} \\ \vdots \\ d_{rn} \end{bmatrix} \tag{9}$$

Now we can rewrite Equation (7) in a more concise way as below:

$$L = \frac{1}{n|\omega|}(\mathbf{D} - \mathbf{X}\boldsymbol{\theta})^{\mathrm{T}}(\mathbf{D} - \mathbf{X}\boldsymbol{\theta}) \tag{10}$$

Equation (10) is actually the linear regression model [26, 27] and its solution is given by:

$$\boldsymbol{\theta} = (\mathbf{X}^{\mathrm{T}}\mathbf{X})^{-1}\mathbf{X}^{\mathrm{T}}\mathbf{D} \tag{11}$$

Although the learning strategy has been given, the training samples are not easy to collect since it is very difficult to accurately measure depths in outdoor scenes with current depth cameras. In order to obtain the accurate depth information as far as possible, we use the dehazing results of Kopf et al. [13] to make an inverse calculation to acquire the depth maps. In [13], Kopf used the city model from Bing to acquire the depths for the New York images and a plain 30-meter digital terrain model for the Yosemite images. We learn the coefficients from the obtained depth maps and their corresponding hazy images according to Equation (11), and a typical learning result is that $\theta_0 = 0.1893$, $\theta_1 = 1.0267$ and

$\theta_2 = -1.2966$. Once values of the coefficients have been determined, they can be used for any single hazy image. These parameters will be used for recovering the scene depth of the hazy image in this paper.

3.4 Estimation of the depth information

As the relationship among the scene depth d, the brightness v and the saturation s has been modelled and the coefficients have been estimated, we can recover the depth map of the given input hazy image according to Equation (5). In Figure 3, we show that the depth maps d and the transmission maps t of the hazy images can be well recovered by the proposed method. With the estimated depth map, the task of dehazing is no longer difficult.

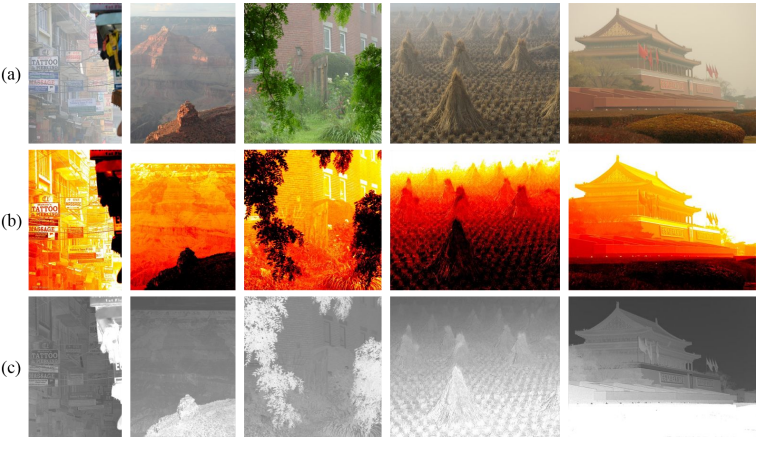

Figure 3: Results of recovering the depth map and the transmission map. (a) Input hazy images. (b) Our recovered depth maps. (c) Our recovered transmission maps.

4 Image Dehazing

4.1 Estimation of the atmospheric light

We have explained the main idea of the method of estimating the atmospheric light in Section 2. In this section, we describe the method in more detail. As the depth map of the input hazy image has been recovered, the distribution of the scene depth is known. Figure 4(a) shows the estimated depth map of the hazy image. Bright regions in the map stand for the distant places.

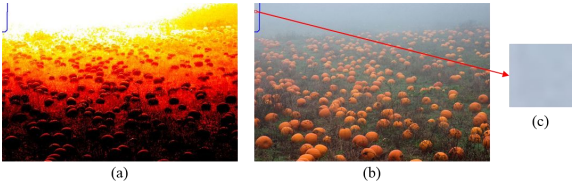

Figure 4: Estimation of the atmospheric light. (a) Our recovered depth map and the brightest region. (b) Input hazy image. (c) The patch from which our method obtains the atmospheric light.

According to Equation (1) and Equation (2), if $d(x) \to \infty$, then $t(x) \to 0$ and $\mathbf{I}(x) = \mathbf{A}$. Based on this theory, we pick the top 0.1 percent brightest pixels in the depth map, and select the pixel with highest intensity in the corresponding hazy image **I** among these brightest pixels as the atmospheric light **A** (see Figure 4(b) and Figure 4(c)).

4.2 Scene radiance recovery

Now that the depth of the scene *d* and the atmospheric light **A** are known, we can estimate the transmission *t* easily according to Equation (2) and recover the scene **J** in Equation (1). For convenience, we rewrite Equation (1) as follows:

$$\mathbf{J}(x) = \frac{\mathbf{I}(\mathrm{x}) - \mathbf{A}}{t(x)} + \mathbf{A} = \frac{\mathbf{I}(\mathrm{x}) - \mathbf{A}}{e^{-\beta d(x)}} + \mathbf{A} \tag{12}$$

where the scattering coefficient β determines the intensity of dehazing indirectly. For avoiding producing too much noise, we restrict the value of the transmission $t(x)$ between 0.1 and 0.9. So the final function used for recovering the scene radiance **J** in the proposed method can be expressed by:

$$\mathbf{J}(x) = \begin{cases} \dfrac{\mathbf{I}(x) - \mathbf{A}}{0.1} + \mathbf{A}, & t(x) \in [0, 0.1) \\ \dfrac{\mathbf{I}(x) - \mathbf{A}}{t(x)} + \mathbf{A}, & t(x) \in [0.1, 0.9] \\ \dfrac{\mathbf{I}(x) - \mathbf{A}}{0.9} + \mathbf{A}, & t(x) \in (0.9, 1] \end{cases} \tag{13}$$

where **J** is actually the haze-free image we want to obtain finally. Figures 5, 6 and 7 show some final results of dehazing of the proposed method.

5 Experiments

In order to verify the effectiveness of the proposed dehazing method, we test it on various hazy images and compare with He et al.'s [16, 17], Tarel et al.'s [21] and Nishino et al.'s [23] methods. All the algorithms are implemented in the MatlabR2013a environment on a P4-3.3GHz PC with 6GB RAM. The parameters we used in the proposed method are initialized as follows: $\beta = 0.95$, $\theta_0 = 0.1893$, $\theta_1 = 1.0267$ and $\theta_2 = -1.2966$. For fair comparison, the parameters used in the three popular dehazing method are set to be optimal according to their original papers ([16, 17], [21] and [23]).

5.1 Qualitative Comparison

Figure 5 shows the comparison between our approach and the method by Tarel et al. [21]. As shown in Figure 5(b), though most of the haze is removed, halo effects appear near the depth discontinuities in the dehazed images (for instance, the leaves at the top region of the first image and the roof of the building in the second image in Figure 5(b)) due to the fact that median filter used in [21] is not an edge-preserving filter. Compared with Tarel et al.'s results, our results are free from the problem of halo effects and the edges of the objects are much sharper as can be seen in Figure 5(c).

Figure 6 shows a comparison between results obtained by [23] and our approach. The dehazed images have high contrast and the details of the scene are well recovered by Nishino et al.'s method as we can see in Figure 6(b). However, the results tend to be

oversaturated and seriously distorted. Our results (see Figure 6(c)), in contrast, are more natural than those in Figure 6(b) obviously.

In Figure 7, we compare our approach with He et al.'s work [16, 17]. The dehazing effects of the two methods are similar to some degree, and the reason can be explained as follows: As the method of recovering the transmission in [16, 17] is based on the dark channel prior, the accuracy of the estimation strongly depends on the validity of the dark channel prior. This prior is invalid when the scene objects are similar to the atmospheric light, leading to the fact that the estimated transmission is not reliable enough in some cases. Different from He et al.'s approach, the transmission is estimated by means of the depth information recovered with the linear color attenuation prior in our approach. Unfortunately, the proposed linear color attenuation prior is also based on statistics that is not sensitive to the scene objects with inherent white color. Therefore, the similarity of the limitation of the two priors determines the fact that the recovered results of the two approaches are similar. Although there is no great difference between the two methods in terms of the dehazing effect, the intensity of dehazing of the proposed method is even stronger and more details can be recovered by our approach as can be seen in Figure 7(c) compared with Figure 7(b).

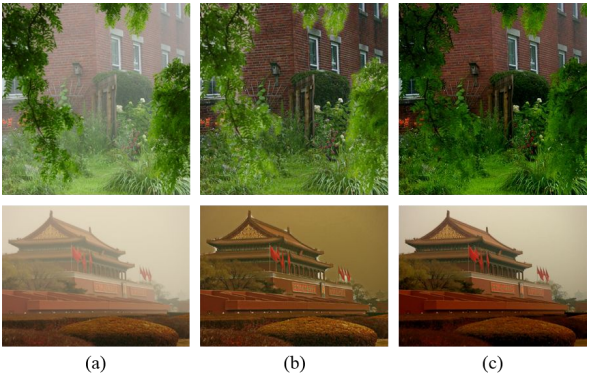

(a) (b) (c)

Figure 5: Comparison with Tarel's work. (a) Input hazy images. (b) Tarel's results. (c) Our results.

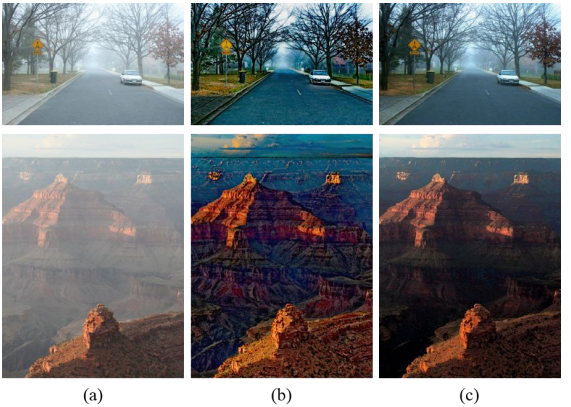

(a) (b) (c)

Figure 6: Comparison with Nishino's work. (a) Input hazy images. (b) Nishino's results. (c) Our results.

Figure 7: Comparison with He's work. (a) Input hazy images. (b) He's results. (c) Our results.

5.2 Quantitative Comparison

For an image of size $m \times n$, the complexity of the proposed dehazing algorithm is only O($m \times n$) when the linear coefficients (θ_0 , θ_1 , θ_2) in Equation (5) are given. In Table 1, we give the time consumption comparison with He et al. [19], Tarel et al. [21] and Nishino et al. [23]. As can be seen, our approach is much faster than others and achieves the real-time requirement.

Image size	He et al.[19]	Tarel et al.[21]	Nishino et al.[23]	Our approach
441×450	9.866 seconds	4.141 seconds	91.661 seconds	**0.559** seconds
600×450	12.228 seconds	8.229 seconds	104.670 seconds	**0.680** seconds
1024×768	36.896 seconds	69.294 seconds	317.386 seconds	**1.757** seconds
1536×1024	73.571 seconds	218.033 seconds	649.722 seconds	**2.999** seconds
1803×1080	90.717 seconds	351.139 seconds	861.360 seconds	**3.534** seconds

Table 1: Time consumption comparison.

6 Conclusion

In this paper, we have proposed a novel color attenuation prior based on the difference between the brightness and the saturation of the pixels within the hazy image. By creating a linear model for the scene depth of the hazy image with this simple but powerful prior and learning the parameters of the model using a supervised learning method, the depth information can be well recovered. By means of the depth map obtained by the proposed method, the scene radiance of the hazy image can be recovered easily. Experimental results show that the proposed approach achieves dramatically high efficiency and outstanding dehazing effect as well.

References

[1] L. Shao, H. Zhang and G. de Haan. An Overview and Performance Evaluation of Classification Based Least Squares Trained Filters. *IEEE TIP*, 17(10): 1772-1782, 2008.

[2] R. Yan, L. Shao and Y. Liu. Nonlocal Hierarchical Dictionary Learning Using Wavelets for Image Denoising. *IEEE TIP*, 22(12): 4689-4698, 2013.

[3] L. Shao, R. Yan, X. Li and Y. Liu. From Heuristic Optimization to Dictionary Learning: A Review and Comprehensive Comparison of Image Denoising Algorithms. *IEEE TCYB*, 44(7): 1001-1013, 2014.

[4] T. K. Kim, J. K. Paik and B. S. Kang. Contrast enhancement system using spatially adaptive histogram equalization with temporal filtering. *IEEE TCE*, 44(1): 82-87, 1998.

[5] SJ. A. Stark. Adaptive image contrast enhancement using generalizations of histogram equalization. *IEEE TIP,* 9(5): 889-896, 2000.

[6] J. Y. Kim, L. S. Kim and S. H. Hwang. An advanced contrast enhancement using partially overlapped sub-block histogram equalization. *IEEE TCSVT,* 11(4): 475-484, 2001.

[7] Y. Y. Schechner and S. G. Narasimhan, and S. K. Nayar. Instant dehazing of images using polarization. In *Proc. CVPR*, 2001.

[8] S. Shwartz, E. Namer, Y. Y. Schechner. Blind haze separation, In *Proc. CVPR*, volume 2, pages 1984-1991, 2006.

[9] S. G. Narasimhan and S. K. Nayar. Chromatic framework for vision in bad weather. In *Proc. CVPR*, 2000.

[10] S. K. Nayar, and S. G. Narasimhan. Vision in bad weather. In *Proc. ICCV*, 1999.

[11] S. G. Narasimhan, and S. K. Nayar. Contrast restoration of weather degraded images. *IEEE TPAMI*, 25(6): 713-724, 2003.

[12] S. G. Narashiman and S. K. Nayar. Interactive deweathering of an image using physical model. *IEEE Workshop on color and photometric Methods in computer Vision*, 6(6.4), 2003.

[13] J. Kopt, B. Neubert, B. Chen, M. Cohen and D. Cohen-Or. Deep photo: Model-based photograph enhancement and viewing. *ACM Transactions on Graphics*, 27(5): 116, 2008.

[14] R. T. Tan. Visibility in bad weather from a single image. In *Proc. CVPR*, 2008.

[15] R. Fattal. Single image dehazing. *ACM Transactions on Graphics*, 27(3), 2008.

[16] K. He, J. Sun, and X. Tang. Single image haze removal using dark channel prior. In *Proc. CVPR*, 2009.

[17] K. He, J. Sun, and X. Tang. Single image haze removal using dark channel prior. *IEEE TPAMI* 33(12): 2341-2353, 2011.

[18] K. He, J. Sun, and X. Tang. Guided image filtering. In *Proc. ECCV*, pages 1-14, 2010.

[19] K. He, J. Sun and X. Tang. Guided image filtering. *IEEE TPAMI*, 35(6): 1397-1409, 2013.

[20] Levin, Anat, L. Dani, and W. Yair. A closed-form solution to natural image matting. *IEEE TPAMI,* 30(2): 228-242, 2008.

[21] J. P. Tarel, and H. Nicolas. Fast visibility restoration from a single color or gray level image. In *Proc. ICCV*, 2009.

[22] L. Kratz, and K. Nishino. Factorizing scene albedo and depth from a single foggy image. In *Proc. ICCV*, 2009.

[23] K. Nishino, L. Kratz, and S. Lombardi. Bayesian defogging. *IJCV*, 98(3): 263-278, 2012.

[24] E. J. McCartney. Optics of the atmosphere: scattering by molecules and particles. *New York, John Wiley and Sons, Inc.* 1976.

[25] S. G. Narasimhan and S. K. Nayar. Vision and the atmosphere. *IJCV*, 48(3): 233-254, 2002.

[26] N. R. Draper and H. Smith. Applied regression analysis. 2nd edn. John Wiley, 1981.

[27] T. Hastie, R. Tibshirani, J. Friedman and T. Hasti. The elements of statistical learning. New York: Springer, 2009.